

Biaxial nonlinear surface waves

Paul B. Lundquist

Department of Physics and Astronomy, The University of Iowa, Iowa City, Iowa 52242

David R. Andersen

Department of Electrical and Computer Engineering, The University of Iowa, Iowa City, Iowa 52242

Pascal Morel

Institut des Sciences de la Matière et du Rayonnement, 6 rue du Maréchal Juin, 14000 Caen, France

(Received 8 July 1996)

In this paper we present calculations describing nonlinear surface waves at the interface between an isotropic nonlinear self-focusing medium and a linear biaxial dielectric. These solutions exhibit self-walk-off in the Poynting vector and elliptical polarization, both of which vary as a function of the distance from the interface. If the dielectric tensor element in the direction perpendicular to the interface has a value that is between the tensor elements in the other two principal directions, then there exists a stop band in the power dispersion curves. This phenomenon is not present when the linear crystal is uniaxial. [S1063-651X(96)12910-X]

PACS number(s): 42.65.Wi

There is a rich literature concerning nonlinear surface waves (NSW), beginning with the original investigation of such waves existing in a structure comprised of a homogeneous linear dielectric bounded by a homogeneous nonlinear self-focusing dielectric [1-4]. These investigations were motivated by experimental evidence suggesting the existence of such a bound state excited by light obliquely incident on the dielectric boundary. Following the initial development various cases have been examined, including multiple dielectric boundaries [5,6], TE- and TM-type waves [7-12], nonlocal [13] and self-defocusing nonlinearities [14,15]. For a good summary of this field, see, e.g., [16]. However, a unifying simplification inherent in all of these investigations has been the assumption that the media exhibit an isotropic dielectric tensor. In such a case the resulting NSW can be divided into TE and TM modes. In this paper, field profiles and dispersion relations are computed for the fundamental and higher-order NSW that exist in anisotropic dielectric media in which the full vector nature of the nonlinear susceptibility must be considered. The resulting NSW are generally elliptically polarized and exhibit a self-walk-off phenomenon.

The anisotropic dielectric NSW problem is an important one, motivated by the fact that strain is present to some degree in all coherently grown crystal systems. The strain, whether tensile or compressive, induces an anisotropy in the dielectric tensor through a modification of the crystal band structure near the boundary. Because all nonlinear integrated optical waveguides involve dielectric boundaries, and many proposed waveguide schemes use coherently grown crystals (e.g., nonlinear waveguides fabricated from the GaAs/AlGaAs semiconductor system) it is very important to understand the impact that this underlying anisotropy has on the characteristics of the NSW.

I. PROBLEM FORMULATION

The geometry for the NSW problem is shown in Fig. 1. A semi-infinite linear anisotropic crystal occupies the half

space described by $y \geq 0$, and a semi-infinite nonlinear isotropic crystal exists in the region $y \leq 0$. The crystal principal axes are denoted by the directions \hat{x} , \hat{y} , and \hat{z} so that the anisotropic crystal is characterized by the dielectric tensor

$$\epsilon_c = \begin{bmatrix} \epsilon_x & 0 & 0 \\ 0 & \epsilon_y & 0 \\ 0 & 0 & \epsilon_z \end{bmatrix}. \tag{1.1}$$

For $y \leq 0$, the nonlinear polarization is described by the following expression:

$$\mathbf{P} = \left[A|\mathbf{E}|^2\mathbf{E} + \frac{B}{2}(\mathbf{E} \cdot \mathbf{E})\mathbf{E}^* \right], \tag{1.2}$$

where $A = 6\chi_{1122}^{(3)}$ and $B = 6\chi_{1221}^{(3)}$ are the nonlinear susceptibility parameters [17]. In this paper, we will consider the case where $A = B$, corresponding to a nonresonant bound elec-

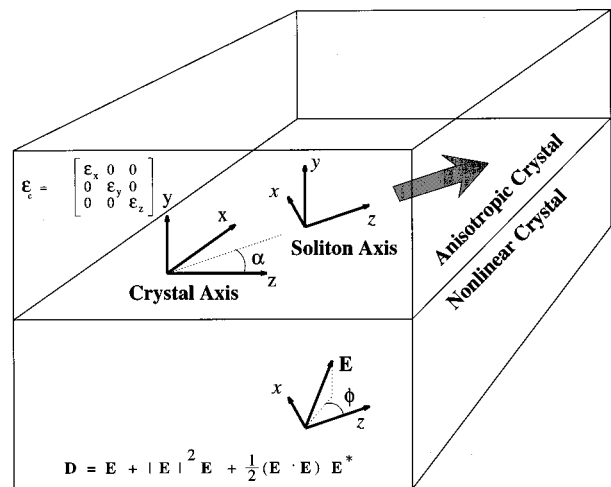


FIG. 1. Anisotropic nonlinear surface-wave problem geometry.

tronic nonlinearity, although the technique described in this paper may be applied for arbitrary A and B .

It is useful to use a coordinate system defined so that one of the axes coincides with the phase propagation direction. The surface-wave directions are denoted with italicized direction variables where the propagation direction $\hat{\mathbf{x}}$ makes an angle α with the principal direction $\hat{\mathbf{x}}$. In this rotated frame of the surface wave, the dielectric tensor must be written as

$$\epsilon_{\text{sw}} = \begin{bmatrix} \epsilon_{\text{xx}} & 0 & \epsilon_{\text{zx}} \\ 0 & \epsilon_y & 0 \\ \epsilon_{\text{zx}} & 0 & \epsilon_{\text{zz}} \end{bmatrix}, \quad (1.3)$$

where the matrix elements are defined as follows:

$$\epsilon_{\text{zz}} = \epsilon_y \cos^2(\alpha) + \epsilon_x \sin^2(\alpha), \quad (1.4)$$

$$\epsilon_{\text{xx}} = \epsilon_y \sin^2(\alpha) + \epsilon_x \cos^2(\alpha), \quad (1.5)$$

$$\epsilon_{\text{zx}} = \frac{(\epsilon_x - \epsilon_y)}{2} \sin(2\alpha). \quad (1.6)$$

Beginning with Maxwell's equations a wave equation can be derived for the NSW field in each of the two dielectrics. The wave equation in the nonlinear medium may be written in normalized form as

$$\nabla \times (\nabla \times \mathbf{E}) = \mathbf{E} + |\mathbf{E}|^2 \mathbf{E} + \gamma (\mathbf{E} \cdot \mathbf{E}) \mathbf{E}^*, \quad (1.7)$$

where γ is the fraction B/A . The corresponding wave equation in the linear anisotropic medium is written in normalized form as

$$\nabla \times (\nabla \times \mathbf{E}) = \epsilon_{\text{sw}} \mathbf{E}, \quad (1.8)$$

All dielectric constants have been normalized by the linear dielectric constant in the nonlinear material (i.e., ϵ in the normalized equations may be less than 1) so that the wave equations are uncluttered by physical constants.

In order to solve the anisotropic NSW problem, the following ansatz is made:

$$\mathbf{E} = \mathcal{E}(y) \exp(inz). \quad (1.9)$$

This form of the solution is assumed in both mediums. Cut-off conditions are found by insisting on exponential extinction of the surface modes far from the interface. These surface modes are used to construct complete solutions by imposing matching boundary conditions at the interface.

II. NONLINEAR ISOTROPIC SURFACE MODES

In the nonlinear medium, the mode profiles may be written in terms of its three components as

$$\mathcal{E} = \begin{bmatrix} U \\ iV \\ W \end{bmatrix}. \quad (2.1)$$

Because the NSW must remain bound to the interface, the real part of the $\hat{\mathbf{y}}$ component of the Poynting vector must be zero. This constraint forces the $\hat{\mathbf{y}}$ component of \mathcal{E} to be in quadrature with the other two field components. As a result the nonlinear Helmholtz wave equation reduces to a set of real equations of motion for the field components U , V , and W :

$$\frac{\partial}{\partial y} U = nQ, \quad (2.2)$$

$$\frac{\partial}{\partial y} V = -\frac{1}{n} \left\{ \frac{\frac{2}{n} (1-\gamma) UV \frac{\partial}{\partial y} U + \frac{2}{n} (1-\gamma) WV \frac{\partial}{\partial y} W + W + (1+\gamma)(W^2 + U^2)W + (1-\gamma)V^2W}{1 + \frac{1}{n^2} (-\beta^2 + (1-\gamma)(W^2 + U^2) + 3(1-\gamma)V^3)} \right\}, \quad (2.3)$$

$$\frac{\partial}{\partial y} W = \frac{1}{n} [-\beta^2 V + (1-\gamma)(W^2 + U^2)V + (1+\gamma)V^3], \quad (2.4)$$

$$\frac{\partial}{\partial y} Q = -\frac{1}{n} [-\beta^2 U + (1+\gamma)(W^2 + U^2)U + (1-\gamma)V^2U], \quad (2.5)$$

where $\beta = \sqrt{n^2 - 1}$ is the linear extinction coefficient in the nonlinear medium far from the interface. In order for the nonlinear solutions to decay to zero β^2 must be greater than zero. This cut-off condition must be considered in addition to linear anisotropic surface-mode cut-off conditions. The set of first-order Eqs. (2.4)–(2.5) can then be integrated using stan-

dard numerical techniques. The initial condition required for the integration consists of the field amplitude at a distance far from the interface on the nonlinear side. This field amplitude must be sufficiently small that the nonlinearity is not manifest. In this limit, the initial condition can be characterized by two parameters: ϕ , shown in Fig. 1, is the polariza-

tion angle of the field with respect to the \hat{z} - \hat{x} plane, and δ parameterizes the field amplitude. Using these two parameters, the initial condition is written $W = \delta \cos(\phi) \exp(\beta y)$, $U = \delta \sin(\phi) \exp(\beta y)$, $V = (n/\beta)W$ and $Q = (\beta/n)U$.

III. BOUNDARY CONDITIONS

Now that a technique for computing the fields on the nonlinear sides of the dielectric interface has been established, I present the method used for matching conditions at the interface. In an anisotropic crystal the field can be written as the sum of two surface modes:

$$\mathbf{E} = [A_+ \mathcal{E}^{(+)} e^{n_y^+ y} + A_- \mathcal{E}^{(-)} e^{n_y^- y}] e^{inz}. \quad (3.1)$$

These surface modes will be discussed in later sections for both uniaxial and biaxial crystals. In either case, the two modes generally have different elliptical polarizations and each mode has its own distinct real evanescent extinction coefficient given by n_y^+ and n_y^- . A linear combination of the two, specified by the coefficients A_+ and A_- , will be necessary to match boundary conditions at the interface. These two mode amplitudes can be related to the \hat{x} and \hat{z} components of the nonlinear field at the interface through the continuity of the tangential electric field:

$$\begin{bmatrix} A_+(y) \\ A_-(y) \end{bmatrix} = \frac{1}{\mathcal{E}_z^{(+)} \mathcal{E}_x^{(-)} - \mathcal{E}_x^{(+)} \mathcal{E}_z^{(-)}} \begin{bmatrix} \mathcal{E}_x^{(-)} & -\mathcal{E}_z^{(-)} \\ -\mathcal{E}_x^{(+)} & \mathcal{E}_z^{(+)} \end{bmatrix} \begin{bmatrix} W(y) \\ U(y) \end{bmatrix}. \quad (3.2)$$

This expression determines the linear-field-mode combination necessary to match the nonlinear field. However, because only the tangential field is considered, it is not sufficient to show that the nonlinear field components match the linear field. In an effort to further simplify the boundary conditions, the following observations are made. The \hat{x} component of the magnetic field will be matched if the \hat{y} component of the electric displacement (\mathcal{D}_y) is matched. The \hat{y} component of the magnetic field is matched as a result of the assumption that the phase velocity for the entire wave is the same, requiring excitations on both sides of the boundary to propagate as $\exp(inz)$. Thus, the problem of matching boundary conditions between the biaxial linear medium and the nonlinear medium reduces to matching the \hat{y} component of the electric displacement (\mathcal{D}_y) and the \hat{z} component of the magnetic field (\mathcal{B}_z). The mismatch in these two components can be expressed as

$$\Delta \mathcal{D}_y(y) = iV[1 + (W^2 + U^2)(1 - \gamma) + V^2(1 + \gamma)] - \epsilon_y(A_+ \mathcal{E}_y^{(+)} + A_- \mathcal{E}_y^{(-)}), \quad (3.3)$$

$$\Delta \mathcal{B}_z(y) = nQ - (A_+ n_y^+ \mathcal{E}_x^{(+)} + A_- n_y^- \mathcal{E}_x^{(-)}) \quad (3.4)$$

The solution technique becomes one of searching the initial condition parameter space for the nonlinear surface mode equations (2.4)–(2.5) to find field distributions for which the mismatches in \mathcal{D}_y and \mathcal{B}_z are simultaneously zero at some location y . The nonlinear Helmholtz equations are integrated numerically using a seventh-order Adams-Bashforth-Moulton scheme [18], and the initial condition amplitude as well as the grid spacing are varied to assure correct results.

For each integration the functions $\Delta \mathcal{D}_y(y)$ and $\Delta \mathcal{B}_z(y)$ can be computed so that by varying the assumed mode index n and angle parameter ϕ the zeros of these two functions can be made to cross. An interface located at the y position of this crossing point then satisfies boundary conditions for the numerically calculated nonlinear surface mode and a linear anisotropic field mode computed from Eqs. (3.2) and (3.1). This process of selecting parameters so that the zero crossings of $\Delta \mathcal{D}_y(y)$ and $\Delta \mathcal{B}_z(y)$ coincide can be performed either visually or automated with an algorithm that follows the gradient of ϕ with respect to the distance between zeros of both functions.

IV. LINEAR ANISOTROPIC SURFACE MODES

The field in the anisotropic medium is assumed to have the form of a linear surface wave

$$\mathbf{E} = \mathcal{E} e^{inz + n_y y}, \quad (4.1)$$

where n is the mode index of the wave and n_y is an evanescent extinction coefficient. Using this assumed form of the field each component of the anisotropic Helmholtz equation (1.8) can be written

$$\mathcal{E}_z \epsilon_{zx} = \mathcal{E}_x (-\epsilon_{xx} n^2 - n_y^2), \quad (4.2)$$

$$\mathcal{E}_z (inn_y) = \mathcal{E}_y (-n^2 + \epsilon_y), \quad (4.3)$$

$$\mathcal{E}_z (\epsilon_{zz} + n_y^2) + \mathcal{E}_x \epsilon_{zx} = \mathcal{E}_y (inn_y). \quad (4.4)$$

By combining Eqs. (4.2) and (4.3) an expression for the anisotropic surface mode can be derived,

$$\mathcal{E} = \begin{bmatrix} \epsilon_{zx}(n - \epsilon_y) \\ -inn_y(n^2 - n_y^2 - \epsilon_{xx}) \\ (n^2 - \epsilon_y)(n^2 - n_y^2 - \epsilon_{xx}) \end{bmatrix} \frac{i\mathcal{E}_y}{nn_y(n^2 - n_y^2 - \epsilon_{xx})} \quad (4.5)$$

However, using Eqs. (4.4) and (4.2) a second expression for the surface mode can be found,

$$\mathcal{E} = \begin{bmatrix} i \frac{nn_y \epsilon_{zx}}{(n^2 - n_y^2 - \epsilon_{xx})(\epsilon_{zz} + n_y^2) + \epsilon_{zx}^2} \\ 1 \\ i \frac{nn_y(n^2 - n_y^2 - \epsilon_{xx})}{(n^2 - n_y^2 - \epsilon_{xx})(\epsilon_{zz} + n_y^2) + \epsilon_{zx}^2} \end{bmatrix} \mathcal{E}_y. \quad (4.6)$$

Because Eqs. (4.5) and (4.6) must be equivalent, the extinction coefficient and the mode index can be related through the equality of \mathcal{E}_z :

$$\frac{n^2 - \epsilon_y}{nn_y} = \frac{nn_y(n^2 - n_y^2 - \epsilon_{xx})}{(n^2 - n_y^2 - \epsilon_{xx})(n_y^2 + \epsilon_{zz}) + \epsilon_{zx}^2}. \quad (4.7)$$

This extinction mode equation can be rearranged into a quadratic polynomial,

$$n_y^4 + \left[\epsilon_z + \epsilon_x - n^2 \left(\frac{\epsilon_y + \epsilon_{zz}}{\epsilon_y} \right) \right] n_y^2 + \left(\frac{n^2 - \epsilon_y}{\epsilon_y} \right) [n^2 \epsilon_{zz} - \epsilon_z \epsilon_x] = 0. \quad (4.8)$$

The two resulting extinction coefficients are then given by the following expressions:

$$\begin{aligned} n_y^{-2} &= \frac{1}{2}(-b - \sqrt{D}), \\ n_y^{+2} &= \frac{1}{2}(-b + \sqrt{D}), \end{aligned} \quad (4.9)$$

where several parameters are defined as follows:

$$D = b^2 - 4c, \quad (4.10)$$

$$b = \left[\epsilon_z + \epsilon_x - n^2 \left(\frac{\epsilon_y + \epsilon_{zz}}{\epsilon_y} \right) \right], \quad (4.11)$$

$$c = \left(\frac{n^2 - \epsilon_y}{\epsilon_y} \right) [n^2 \epsilon_{zz} - \epsilon_z \epsilon_x]. \quad (4.12)$$

V. BIAXIAL NONLINEAR SURFACE WAVES

All the general features of uniaxial nonlinear surface waves discussed in [19,20], such as self-walk-off, elliptical polarization, and angle-tuned cut-off still arise. In addition to these effects, interesting features resulting from the behavior of the discriminant D will be discussed.

In order to have a surface wave, the extinction coefficients are required to be real and less than zero. Though it might seem that a surface wave could have complex extinction coefficients, this is not the case. It can be shown that complex extinction coefficients lead to a real component of the Poynting vector perpendicular to the interface. Since power cannot flow away from the interface in a stable surface wave, the extinction coefficients cannot have a complex component.

The requirement that the squared extinction constants are both real and greater than zero lead to three conditions. The first condition, $b < 0$, is a cut-off corresponding to the occurrence where both modes become plane waves. The second condition $c > 0$ is a cut-off corresponding to the case where only one mode becomes a plane wave. The third condition $D > 0$ describes a forbidden band of parameters where the extinction coefficients become complex. This stop band does not occur in the analogous uniaxial surface wave problem.

The cut-off conditions that $b < 0$ and $c > 0$ define three critical curves:

$$\eta_1^2 = \epsilon_y, \quad (5.1)$$

$$\eta_2^2 = \frac{\epsilon_z \epsilon_x}{\epsilon_{zz}}, \quad (5.2)$$

$$\eta_3^2 = \frac{\epsilon_z + \epsilon_x}{\epsilon_y + \epsilon_{zz}} \epsilon_y. \quad (5.3)$$

These curves describe a general cut-off condition $n^2 > \max[\eta_1^2, \eta_2^2, \eta_3^2]$, which can depend on the launch angle α through ϵ_{zz} in η_2 and η_3 . Though it may seem that the cut-off requirements could also be satisfied if $\eta_3^2 < n^2 < \min[\eta_1^2, \eta_2^2]$, a consideration of each ensuing special case shows that these inequalities do not have solutions.

Analysis of the stop band is aided by writing D as a quadratic in n^2 ,

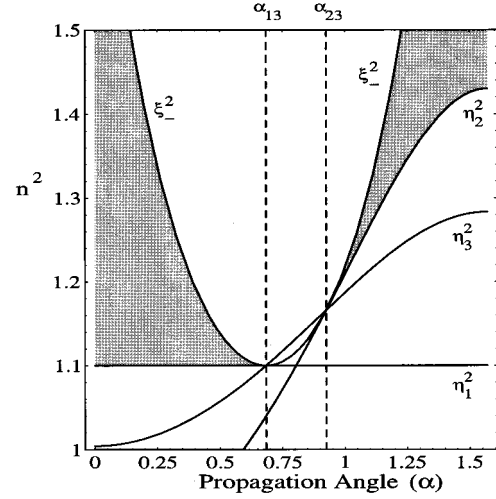


FIG. 2. Biaxial surface-wave cut-off and stop band for the case where $\epsilon_x=0.88$, $\epsilon_y=1.1$, and $\epsilon_z=1.43$. The grey region shows an allowed band of values for n^2 as a function of the direction of propagation (α). Surface waves in this band are not allowed to propagate between the angles α_{13} and α_{23} .

$$D = \tilde{a}n^4 + \tilde{b}n^2 + \tilde{c}, \quad (5.4)$$

where the coefficients of the quadratic may be expressed as follows:

$$\tilde{a} = \left[\frac{\epsilon_{zz} - \epsilon_y}{\epsilon_y} \right]^2, \quad (5.5)$$

$$\tilde{b} = \frac{2}{\epsilon_y} [(2\epsilon_y - \epsilon_z - \epsilon_x)\epsilon_{zz} + 2\epsilon_z\epsilon_x - (\epsilon_z + \epsilon_x)\epsilon_y], \quad (5.6)$$

$$\tilde{c} = (\epsilon_z - \epsilon_x)^2. \quad (5.7)$$

When this quadratic has real roots ξ_{\pm}^2 , then $D < 0$ between them. Hence, the band of n^2 values between the roots are forbidden. If D has only complex roots then no such band will occur. The roots of D can be written as follows:

$$\xi_{\pm}^2 = \frac{-\tilde{b} \pm \sqrt{\tilde{D}}}{2\tilde{a}}, \quad (5.8)$$

$$\tilde{D} = \left(\frac{2}{\epsilon_y} \right)^2 (\epsilon_z - \epsilon_x)^2 (\epsilon_z - \epsilon_y) (\epsilon_y - \epsilon_x) \sin^2(2\alpha). \quad (5.9)$$

The form of \tilde{D} shows that the roots of D can only be real if ϵ_y is between the values of ϵ_x and ϵ_z .

A. Case 1: $\epsilon_x < \epsilon_y < \epsilon_z$

There are three cases corresponding to the ordering of the principal dielectric tensor constants. In the first case the dielectric constant perpendicular to the surface is between the principal dielectric constants in the other two directions. Without loss of generality, the ordering can then be assumed to be as follows: $\epsilon_x < \epsilon_y < \epsilon_z$. Figure 2 illustrates the angle dependence of the cut-off relations and stop band in the following discussion for a specific example where $\epsilon_x=0.88$, $\epsilon_y=1.1$, and $\epsilon_z=1.43$.

If α is 0 or $\pi/2$ the surface wave is propagating along a principal axis and both ξ_{\pm} converge to the same value. In

particular these values are given by the following expressions:

$$\xi_{\pm}^2(0) = \frac{\epsilon_y(\epsilon_z - \epsilon_x)}{(\epsilon_z - \epsilon_y)}, \quad (5.10)$$

$$\xi_{\pm}^2(\pi/2) = \frac{\epsilon_y(\epsilon_x - \epsilon_z)}{(\epsilon_x - \epsilon_y)}. \quad (5.11)$$

The upper curve ξ_+^2 becomes infinite when $\tilde{a}=0$, which occurs at an angle $\alpha=\theta$ such that

$$\sin^2(\theta) = \frac{\epsilon_z - \epsilon_y}{\epsilon_z - \epsilon_x}. \quad (5.12)$$

At this angle the forbidden band extends from ξ_-^2 to ∞ .

With this ordering of the dielectric constants, the correct cut-off relations are found by determining the angles at which the critical curves coincide. Given this information and the maximum critical curve at the angles $\alpha=0$ and $\alpha=\pi/2$ the cut-off relations in three resulting ranges of α are determined. The following expressions define the angles α_{jk} where the curves η_j^2 and η_k^2 cross:

$$\sin^2(\alpha_{13}) = \frac{\epsilon_x - \epsilon_y}{\epsilon_x - \epsilon_z}, \quad (5.13)$$

$$\sin^2(\alpha_{12}) = \frac{\epsilon_z(\epsilon_x - \epsilon_y)}{\epsilon_y(\epsilon_x - \epsilon_z)}, \quad (5.14)$$

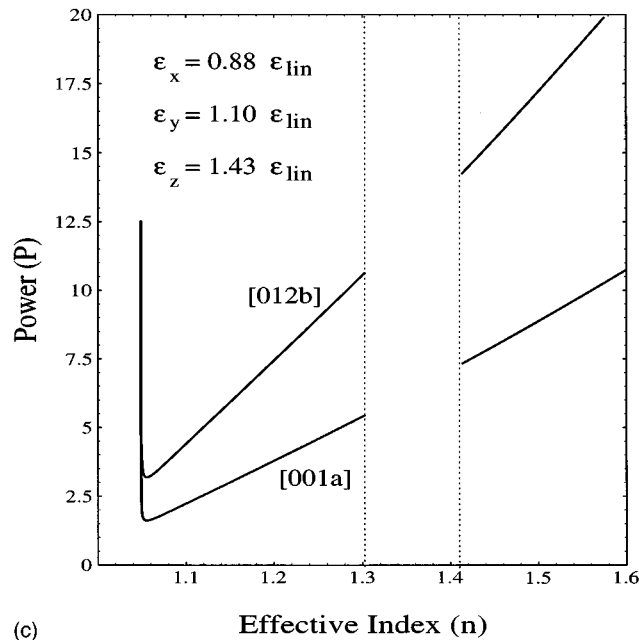
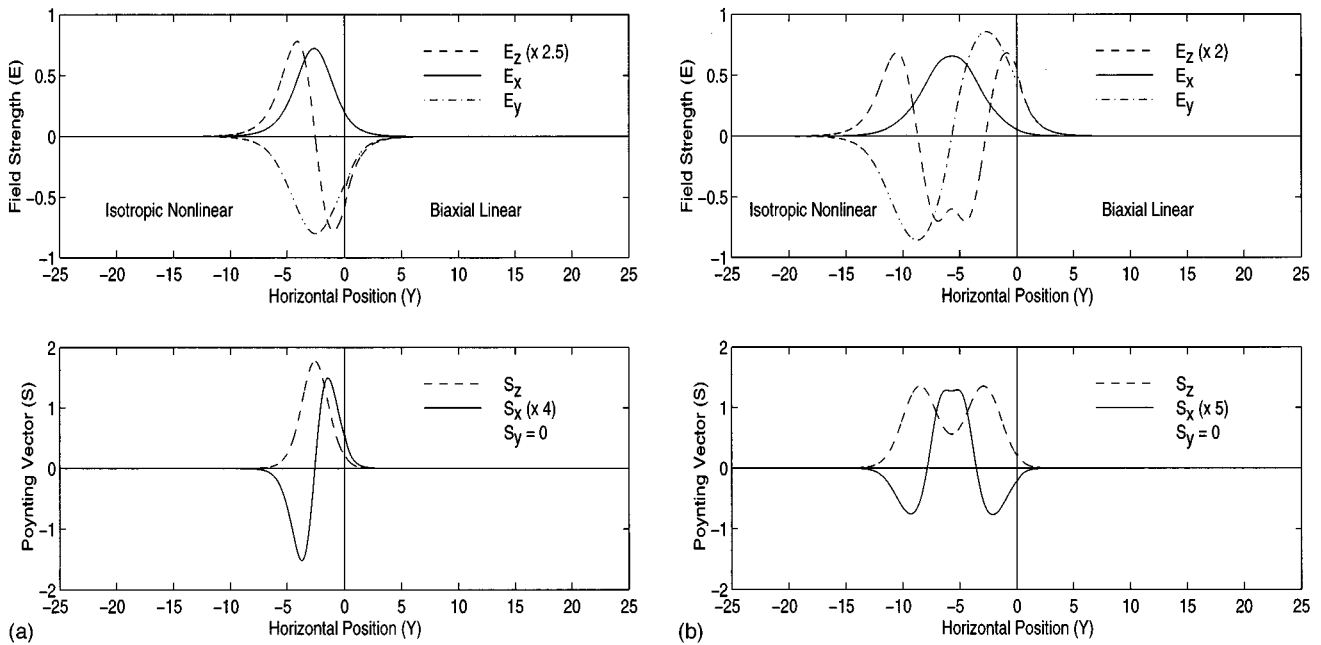


FIG. 3. Biaxial nonlinear surface-wave profiles and power dispersion curves for $\epsilon_x=0.88$, $\epsilon_y=1.1$, $\epsilon_z=1.43$, and $\alpha=1.4$; (a) [001a] mode for $n^2=1.68$, (b) [012b] mode for $n^2=1.5$, (c) power dispersion curves for the [001a] and [012b] modes.

$$\sin^2(\alpha_{23}) = \frac{\epsilon_z^2(\epsilon_x - \epsilon_y)}{[\epsilon_y(\epsilon_z + \epsilon_x) - \epsilon_z\epsilon_x](\epsilon_x - \epsilon_z)}. \quad (5.15)$$

Since $\sin^2(\alpha)$ is an increasing function in the considered range of angles, it can be shown that $\alpha_{13} < \alpha_{12} < \alpha_{23}$. By comparing each of the curves at $\alpha=0$ and $\alpha=\pi/2$ it can be concluded that at angles between 0 and α_{13} the cut-off relation is $n^2 > \eta_1^2 = \epsilon_y$. This cut-off condition has no angle dependence, just as in isotropic surface modes. Between the angles $\alpha = \alpha_{23}$ and $\alpha = \pi/2$ the maximal critical curve is η_2^2 so that the cut-off is given as follows:

$$n^2 > \eta_2^2 = \frac{\epsilon_z\epsilon_x}{\epsilon_z\cos^2(\alpha) + \epsilon_x\sin^2(\alpha)}. \quad (5.16)$$

This expression is exactly the cut-off that occurs for uniaxial surface waves when $\epsilon_z = \epsilon_y$.

Between the angles α_{13} and α_{23} the maximal critical curve is η_3^2 . However, recalling that the curve $n^2 = \eta_3^2$ corresponds to the case when $b=0$ and the other two critical curves represent the case where $c=0$, it is apparent that the intersection of these two curves must also intersect one of the stop band edges ξ_{\pm} . Since both $\xi_{\pm}^2(0)$ and $\xi_{\pm}^2(\pi/2)$ can be shown to be greater than η_1^2 or η_2^2 at the angles 0 and $\pi/2$, it follows that the lower edge of the stop band (described by the curve $n^2 = \xi_{-}^2$) dips below cut-off between $\alpha = \alpha_{13}$ and $\alpha = \alpha_{23}$. Hence, solutions can exist only if $n^2 > \xi_{+}^2$ in this angle range.

In Figs. 3(a) and 3(b), the electric field and Poynting vector profiles for the [001a] and [012b] modes are illustrated. These modes exhibit self-walk-off and y -dependent elliptical

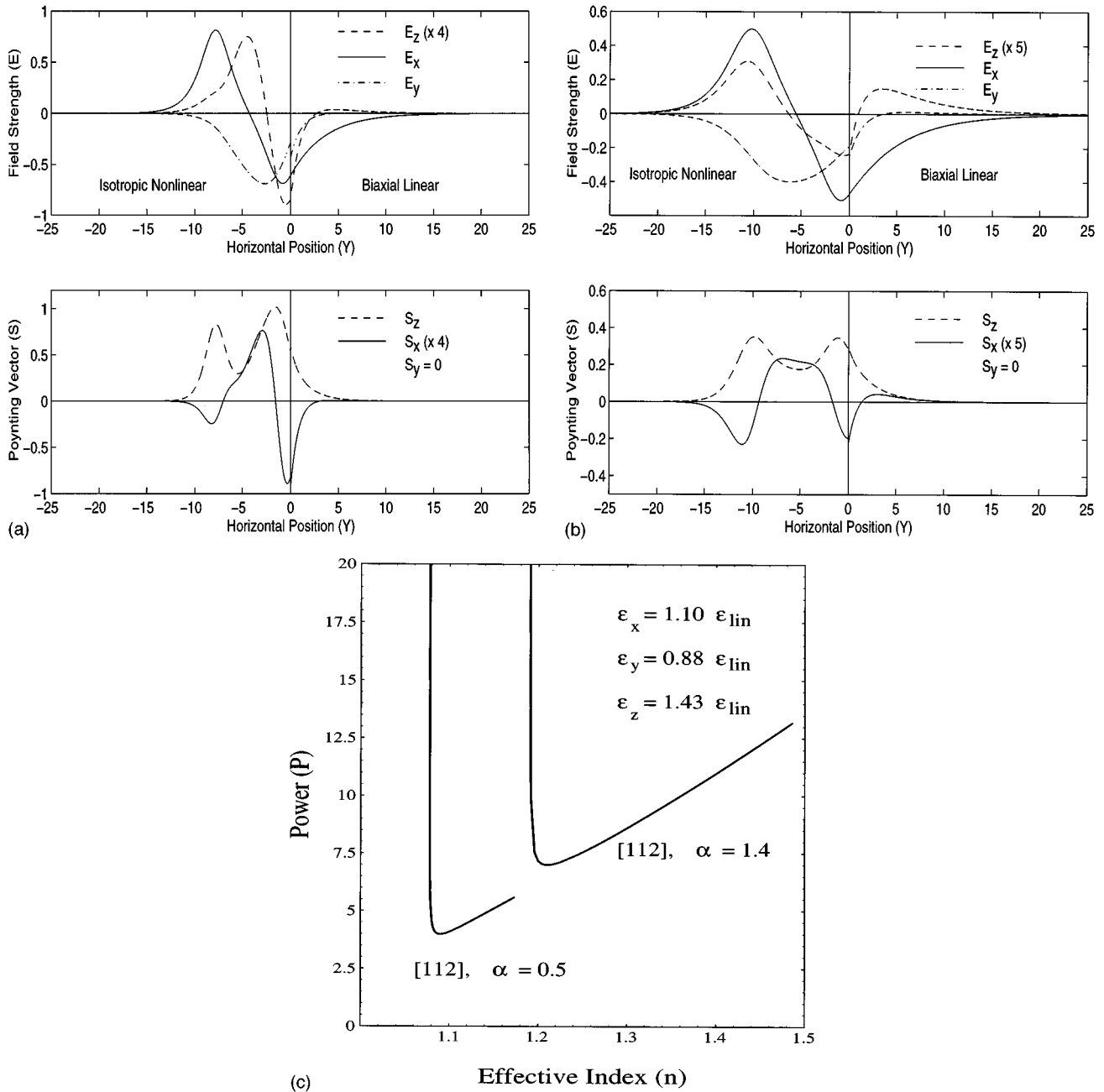


FIG. 4. Biaxial nonlinear surface-wave profiles and power dispersion curves for $\epsilon_y=0.88$, $\epsilon_x=1.1$, $\epsilon_z=1.43$: (a) [112] mode for $\alpha=1.4$ and $n^2=1.5$, (b) [112] mode for $\alpha=0.5$ and $n^2=1.2$, (c) power dispersion curves for the [112] mode the angles $\alpha=0.5$ and $\alpha=1.4$.

polarization [20]. In Fig. 3(c), power dispersion curves and a stop band are shown for these two modes.

B. Case 2: $\epsilon_y < \epsilon_x < \epsilon_z$

When the dielectric tensors are ordered so that $\epsilon_y < \epsilon_x < \epsilon_z$ the curve η_2^2 curve is never any smaller than ϵ_x . It follows that η_1^2 cannot be the maximal cut-off curve. By showing that η_2^2 and η_3^2 cannot coincide for any value of α and then considering their relative values at $\alpha=0$ and $\alpha=\pi/2$ it can be shown that $\eta_2^2 > \eta_3^2$. It follows that the cut-off relation with this dielectric constant ordering is always $n^2 > \eta_2^2$, which may also be written as follows:

$$n^2 > \frac{\epsilon_z \epsilon_x}{\epsilon_z + (\epsilon_x - \epsilon_z) \sin^2(\alpha)}. \quad (5.17)$$

This cut-off relation also occurs in a uniaxial surface wave when $\epsilon_z = \epsilon_y$.

Figures 4(a) and 4(b) illustrate the electric field and Poynting vector profiles of the [112] mode at $\alpha=0.5$ with $n^2=1.2$ and the same mode for $\alpha=1.4$ with $n^2=1.5$. The corresponding power dispersion curves are shown in Fig. 4(c). It can be seen from this illustration how by increasing the angle-tuned cut-off the power threshold can also be increased.

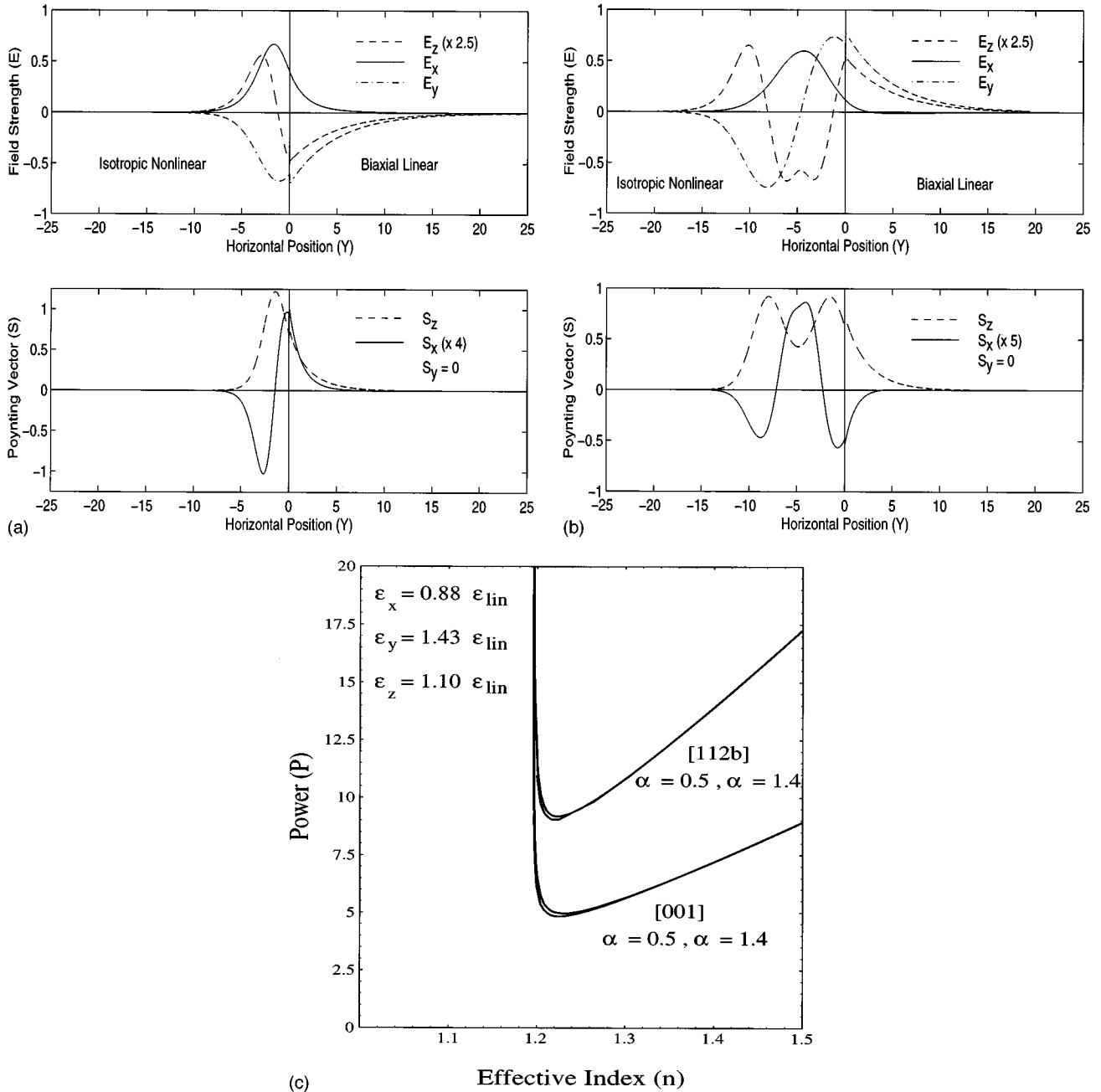


FIG. 5. Biaxial nonlinear surface-wave profiles and power dispersion curves for $\epsilon_y=1.43$, $\epsilon_x=0.88$, $\epsilon_z=1.1$: (a) [001] mode for $n^2=1.5$, (b) [112b] mode for $n^2=1.5$, (c) power dispersion curves for the [112b] and [001] mode and the angles $\alpha=0.5$ and $\alpha=1.4$.

C. Case 3: $\epsilon_y > \epsilon_z > \epsilon_x$

If instead the dielectric constants are ordered so that ϵ_y is greater than the dielectric constants in the other directions, then the curve $n^2 = \eta_1^2$ will always be greater than the other two critical cut-off curves. In this case the cut-off is given simply by $n^2 > \epsilon_y$. As in an isotropic medium this cut-off has no angle dependence. The Poynting vector and electric-field profile are illustrated for the [001] and [112b] modes in Figs. 5(a) and 5(b), respectively. Power dispersions for these two modes at both angles $\alpha=0.5$ and $\alpha=1.4$ are illustrated in 5(c). This demonstrates the angle independence of the cut-off for this configuration. Though the cut-off for these solutions is angle independent, the surface waves still have a small dependence on the propagation direction. This angle dependence of the modes in this configuration is most apparent at the power threshold where a difference in the power dispersion curves at the two angles can be detected.

VI. COMPARISON TO UNIAXIAL NONLINEAR SURFACE WAVES

In Ref. [20] we presented the case corresponding to a uniaxial crystal. In this section we show how those solutions exist as a limiting case of the solutions presented in the current paper.

There are two distinct possible crystal orientations for a uniaxial crystal with one of its principal axes perpendicular to the interface. In the first case, if $\epsilon_z = \epsilon_x$ the problem loses all dependence on the direction of propagation because any components of the electric field parallel to the interface induce the same relative polarization. Therefore, this case is essentially the same as the isotropic surface-wave problem. Consequently, we concentrate on the crystal orientation where $\epsilon_z = \epsilon_y$.

The discriminant D in Eq. (4.10) can also be expressed as follows:

$$D = \left[n^2 \left(\frac{\epsilon_{zz} - \epsilon_y}{\epsilon_y} \right) + (\epsilon_z - \epsilon_x) \right]^2 + 4n^2 \frac{(\epsilon_y - \epsilon_z)(\epsilon_{zz} - \epsilon_x)}{\epsilon_y}. \quad (6.1)$$

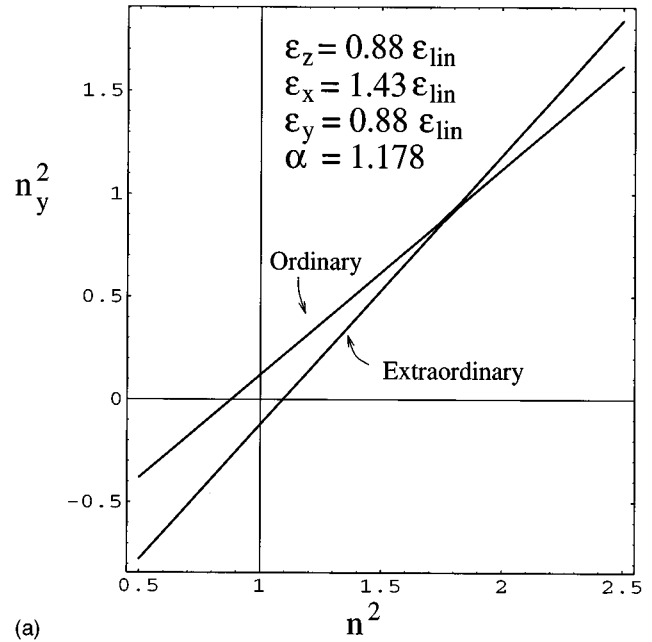
For the uniaxial case, the square root of the discriminant is given by

$$n^2 \left(\frac{\epsilon_{zz} - \epsilon_y}{\epsilon_y} \right) + (\epsilon_z - \epsilon_x) \quad (6.2)$$

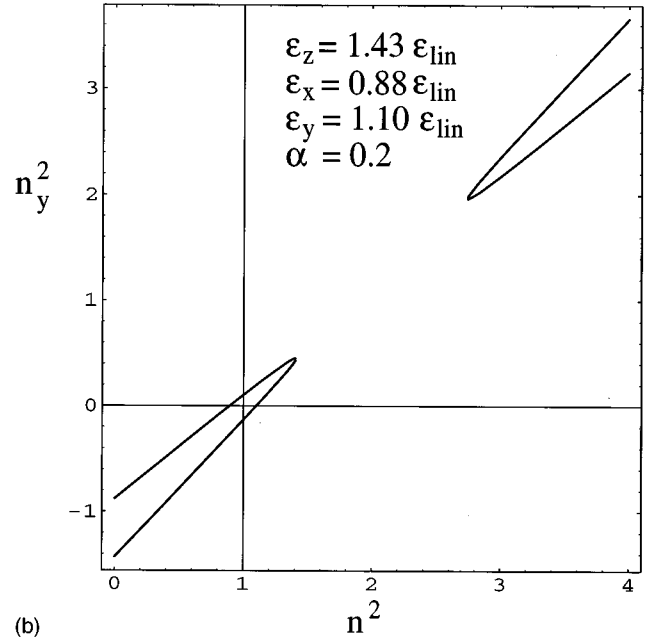
so that the expressions for the extinction coefficients in Eqs. (4.9) can be reduced to the much simpler uniaxial surface-mode extinction coefficients. The solution that depends on the propagation angle through ϵ_{zz} is recognized as the extraordinary mode extinction number $n_y^{(e)}$, while the solution that is independent of the propagation angle is recognized as the ordinary extinction number $n_y^{(o)}$:

$$n_y^{(e)2} = n^2 \frac{\epsilon_{zz}}{\epsilon_y} - \epsilon_x, \quad (6.3)$$

$$n_y^{(o)2} = n^2 - \epsilon_x. \quad (6.4)$$



(a)



(b)

FIG. 6. Plots of the squared extinction coefficients as a function of the squared effective mode index: (a) For the uniaxial crystal parameters $\epsilon_x=1.43$, $\epsilon_y=0.88$, and $\alpha=1.178$, (b) for the biaxial crystal parameters $\epsilon_x=0.88$, $\epsilon_y=1.1$, $\epsilon_z=1.43$, and $\alpha=0.2$.

The corresponding mode polarizations $\mathcal{E}^{(o)}$ and $\mathcal{E}^{(e)}$ can be found from Eq. (4.5) using $n_y = n_y^{(o)}$ for the ordinary mode and using $n_y = n_y^{(e)}$ for the extraordinary mode.

For both modes, the squared uniaxial extinction coefficient, n_y^2 , is a linear function of the squared effective mode index n^2 . This is illustrated in Fig. 6(a). Both linear modes are required to have real extinction coefficients and n^2 is required to be greater than 1. Because the zero of the extraordinary curve is larger than either 1 or the zero of the ordinary curve, the extraordinary mode determines the cut-off for the uniaxial solutions for the parameters used in Fig. 6(a). The $n_y^{(e)2}$ and $n_y^{(o)2}$ lines generally cross and can be understood as

a limiting case of hyperbola solutions to Eq. (4.8). For biaxial crystals the hyperbola curves consist of two disconnected parts, giving rise to phenomena that differ from the uniaxial case. In particular, for the crystal orientation given by the dielectric element ordering $\epsilon_x < \epsilon_y < \epsilon_z$, the major axis direction for the hyperbola in the $n^2 - n_g^2$ plane explains the stop-gap phenomena discussed earlier. This is illustrated in Fig. 6(b). For crystal orientations where the dielectric constant in the y direction is smaller or greater than both of the other principal tensor elements, the direction of the hyperbola major axis is such that no stop band arises.

VII. SUMMARY

In this paper we have described analysis leading to calculations of biaxial NSW Electric-field profiles and Poynting vectors for the lowest-order modes were presented, and power-dispersion curves were illustrated. These surface waves exhibit the self-walk-off phenomena, where the Poynting vector direction is mostly in the direction of phase propagation, but has a small transverse component parallel to

the interface. This transverse component varies with the distance from the interface. Each of the solutions were elliptically polarized and the polarization varied as a function of the transverse coordinate normal to the interface plane. Expressions for the angle-tuned cutoff of anisotropic NSW's have also been presented. The solution regimes for biaxial surface waves were classified and discussed in detail. The solutions arising from a biaxial crystal differs from those of uniaxial crystals presented in [20,19] primarily because biaxial crystals can lead to a stop-gap in the surface-wave-mode index.

One of the phenomena in the biaxial case that sets it apart from the uniaxial case is the surface-wave stop band. This is a consequence of extinction coefficients becoming complex and differs from typical cut-offs where extinction coefficients become purely imaginary. This can also be understood as a deformation of curves describing the uniaxial decay coefficients for nearly degenerate polarization modes so that the decay coefficients are described by equations for hyperbolas rather than lines.

-
- [1] A. G. Litvak and V. A. Mironov, *Izv. Vyssh. Uchenbyn. Zaved. Radiofiz.* **11**, 1911 (1968).
 - [2] W. J. Tomlinson, *Opt. Lett.* **5**, 323 (1980).
 - [3] A. A. Maradudin, *Z. Phys. B* **41**, 341 (1981).
 - [4] N. Akhmediev, *Sov. Phys. JETP* **57**, 1111 (1983).
 - [5] A. D. Boardman and P. Egan, *IEEE Journal Quantum Electron.* **QE-22**, 319 (1986).
 - [6] N. Akhmediev, A. Antkiewicz, and H. Tran, *J. Opt. Soc. Am. B* **10**, 230 (1993).
 - [7] A. D. Boardman *et al.*, *Phys. Rev. A* **35**, 1159 (1987).
 - [8] D. Mihalache *et al.*, *Opt. Lett.* **12**, 187 (1987).
 - [9] S. W. Kang, *J. Lightwave Technol.* **13**, 391 (1995).
 - [10] J. Jasinski and K. Gniadek, *Opt. Quantum Electron.* **26**, 865 (1994).
 - [11] H. Hayata, M. Nagai, and M. Koshiba, *Electron. Lett.* **23**, 1305 (1987).
 - [12] A. D. Boardman and T. Twardowski, *Phys. Rev. A* **39**, 2481 (1989).
 - [13] A. B. Aceves *et al.*, *J. Opt. Soc. Am. B* **7**, 963 (1990).
 - [14] S. R. Skinner and D. R. Andersen, *J. Opt. Soc. Am. B* **8**, 759 (1991).
 - [15] D. R. Andersen and S. R. Skinner, *J. Opt. Soc. Am. B* **8**, 2265 (1991).
 - [16] *Nonlinear Surface Electromagnetic Phenomena*, edited by H. E. Ponath and G. Stegeman (North-Holland, Amsterdam, 1991).
 - [17] P. D. Maker and R. W. Terhune, *Phys. Rev. A* **137**, A801 (1965).
 - [18] L. Shampine and M. Gordon, *Computer Solutions of Ordinary Differential Equations* (W. H. Freeman, San Francisco, 1975).
 - [19] L. Toner *et al.*, *Electron. Lett.* **29**, 1186 (1993).
 - [20] P. B. Lundquist and D. R. Andersen, *Phys. Rev. E* **53**, 4077 (1996).